Pergamon

Int. J. Solids Structures Vol. 34, Nos. 35–36, pp. 4557–4579, 1997

0020–7683/97 $17.00 + .00

PII: S0020–7683(97)00038–3

AN INTEGRAL EQUATION FOR CHANGES IN THE STRUCTURAL DYNAMICS CHARACTERISTICS OF DAMAGED STRUCTURES

H. LUO and S. HANAGUD
School of Aerospace Engineering, Georgia Institute of Technology, Atlanta, GA 30332, U.S.A.

(*Received* 9 *July* 1996; *in revised form* 13 *January* 1997)

Abstract—This paper presents a relationship between the structural dynamic characteristics of damaged and intact structures. Such a relationship is derived in the form of an integral equation and is used to develop a method of flaw identification. The resulting flaw identification procedure uses the experimental data and relates the flaw to the observed structural dynamic response. The algorithm enables one to detect the damage locations and the corresponding damage magnitude simultaneously. Numerical simulations and experiments are conducted to validate the theory. © 1997 Elsevier Science Ltd.

1. INTRODUCTION

Flaw detection in structural systems in an active research area. The conventional health monitoring of structures is based on traditional nondestructive evaluation/testing (NDE/T) methods such as radiography, ultrasonics, acoustic emission, optical methods, thermal methods, magnetic methods, and eddy current test, etc. With advances in computer science and technology, the integration of NDE/T instruments with microprocessors has enhanced the flexible signal processing capability and fast data storing and retrieving capability, and thus making many of the traditional NDE/T methods more efficient, for example the research reported by Frankle (1993) and Kreier *et al.* (1993). Despite the well-documented successes of NDE/T methods, most of the conventional NDE/T methods have drawbacks and limitations. Usually, conventional NDE/T methods are local in nature, passive and labor intensive. Very often, special auxiliary instruments and expert explanation are required.

Flaw detection based on structural dynamic response and system identification techniques is another choice. Currently, this is a very active research area. Methods reported in the literature can be classified into three categories: experimental-data-based methods, model-based methods and model-free methods based on neural networks and expert systems.

Experimental-data-based methods

Experimental-data-based detection methods use only structural dynamic characteristics generated by test data. By comparing identified structural dynamic characteristics of the structure in an intact state with those from the structure at a later date in service, the damage locations and damage magnitudes are inferred through mathematical manipulations. The measured or identified data can be in the form of natural frequencies (Cawley and Adams 1979a; Pabst and Hagedorn 1993), damping ratios (Lee *et al.* 1987; Griffin *et al.* 1991) mode shapes (Cempel *et al.* 1992), and curvature mode shapes (Pandey *et al.* 1991) etc. The advantage of the experimental data-based methods is that a mathematical model like a refined finite element model of the structure is not required.

Model-based methods

Finite element model-based detection methods are based on the finite element model (FEM) refinement technique. In model-based methods, it is assumed that an FEM of the

structure is available before damage has occurred and the FEM and the experimental modal analysis model (EMA) can be matched under certain criteria for the undamaged structure. The existence of significant damages in the structure will result in changes of structural dynamic characteristics such as frequencies, damping ratios and mode shapes. By comparing the identified data from the measurement of the post-damaged structure and the data from the calculation of the refined intact FEM, the resulting discrepancy is determined and used to detect the existence of the flaw, the location of the flaw, and assess the extent of the damages in the structure. The algorithms for model-based detection methods can be broadly classified into three classes: optimal matrix modifications (e.g. Rodden 1968; Kabe 1985; Smith and Beattie 1991), sensitivity-based updates (e.g. Collins *et al.* 1974; Lin 1993), and eigenstructure assignment techniques (e.g. Minas and Inman 1990; Zimmerman and Kaouk 1992; Lim 1995). The application of model-based methods has many problems. Usually the FEM degrees of freedom are very large while the EMA degrees-of-freedom are very small. In modal based methods, either FEM degrees-of-freedom are reduced or EMA degrees-of-freedom are increased. Both these procedures lead to errors and loss of physical interpretability. In addition, manipulation large degrees-of-freedom FEM renders the method not practical for real time identification of damage.

Model-free methods

Model-free detection methods are also known as experience-based detection methods. The popular algorithms in this category include rule-based expert systems (ES) and artificial neural networks (ANN) (Wu *et al.* 1992; Worden *et al.* 1993; Manning 1994; Rhim and Lee 1995). Most of the structural flaw identification researches in the literature are limited to lab models and numerical simulations. The application of model-free methods to the health monitoring in a real structure is still facing the challenges from the robustness of the scheme and the efficiency in the neural network training procedures, etc. Our objective is to improve the accuracy of the experimental data based method. We have developed an integral equation model that can be used with experimentally generated data to provide an accurate damage information.

2. IMPROVEMENTS OF EXPERIMENTAL-DATA BASED METHODS

In practice, experimental-data-based methods are still preferred because of their simplicity. There are many attempts to improve the accuracy of this method without resorting to the use of the complicated FEM. First attempts to improve the experimental-data based methods used the measured or identified natural frequency changes with receptance analysis (Adams *et al.* 1978), sensitivity analysis (Cawley and Adams, 1979a, 1979b) and rank ordering of frequency shifts (Armon *et al.* 1991). As applied to composites, experimentally detected frequency or stiffness changes and changes in damping ratios were used by Adams *et al.* (1975) and Mantena (1986). More recently, Griffin and Sun (1991) demonstrated a flaw location procedure for composite beams by using damping changes and strain energy distribution in vibration modes.

The next step was to consider modes in addition to frequency and damping ratios. The enhanced sensitivity of curvature mode shapes to damage was demonstrated by Pandey *et al.* (1991). Pabst and Hagedorn (1993) proposed a procedure that used Rayleigh quotient to relate flaws (modeled as stiffness losses) to experimentally determined frequency changes. In using the Rayleigh quotients, Pabst and Hagedorn assumed that the mode shapes of a structure in intact and damaged states are the same and interchangeable. However, the curvature mode information, which is the second derivative of the mode shape, was used in their detection procedure. The effect of change of mode shapes may be significant in damage detection problem because perturbation of dynamic characteristics due to damage may be of the same order. Thus, while using curvature mode information, it is necessary to reexamine the effect of curvature mode changes because they are more sensitive to damages. Similar to the work reported by Pabst and Hagedorn (1993), Cempel *et al.* (1992) assumed that the flaw introduces a perturbation in the stiffness operator with negligible changes of the normal mode shape, but distinct changes in frequencies.

3. PROBLEM SETTING

On the basis of the published literature, we can conclude the following. At present, a rigorous mathematical relation between changes in structural dynamic characteristics of damaged and undamaged structures is not available. Some of the proposed methods can detect only partial damage information like flaw existence or flaw locations or the flaw magnitude. In some other methods, the flaw location and flaw magnitude are obtained separately (one at a time). In papers of Pabst and Hagedorn (1993) and Cempel *et al.* (1992) an assumption was made that the curvature mode shape changes before and after the damage were very small. The mode shapes and curvatures of the damaged structure were assumed to be the same as the corresponding intact structure in both references. The effect of this assumption is studied in this paper.

The objective of this paper is to develop a flaw detection algorithm which is based on experimentally identified data and a rigorous mathematical relation between the flaw information and changes in structural dynamic characteristics including mode shapes. In our work, we assume that the curvature mode shapes of the intact and the damaged structures are different. Both the frequency information and curvature mode shape information are used in the detection algorithm.

4. THEORY

4.1. *Basic assumptions*

In the ensuing discussion of this paper, the following assumptions are made:

(1) Damages to the system can be modeled as a perturbation of ΔL on the linear operator L of the structural differential equations, that is, a stiffness variance in the system.
(2) The undamaged system is stable and the perturbation due to damage does not affect the stability of the system, that is, the presence of damage causes only small perturbations in eigenvalues and eigenfunctions of the system.
(3) Damages occur within the domain of the system, namely, the boundary conditions remain unchanged due to the damages. That is, all the eigenfunctions of the intact structure are comparison functions of the damaged structure. Thus, any eigenfunction of the damaged structure can be expressed as a linear combination of the intact eigenfunctions.

4.2. *Detection theory*

Assuming that the eigenvalue problem of an undamaged structure can be written as

$$L[W(X)] - \lambda M[X]W(X) = 0 \tag{1}$$

with appropriate boundary conditions. In eqn (1), L is a linear homogeneous differential operator; M is a function of spatial variable X; λ is a parameter; $W(X)$ is the displacement in terms of spatial variable X.

Assuming the eigensolutions of eqn (1) are λ_i and ϕ_i, $i = 1,2,\ldots,$ which satisfy eqn (1) for an intact or undamaged system, we have

$$L[\phi_i(X)] - \lambda_i M[X]\phi_i(X) = 0 \tag{2}$$

and the orthogonality conditions

$$k_{ij} = \int_\Omega \phi_i(X) L[\phi_j(X)]\, \mathrm{d}\Omega = \lambda_i \delta_{ij} \tag{3}$$

$$m_{ij} = \int_\Omega \phi_i(X) M(X) \phi_j(X)\, \mathrm{d}\Omega = \delta_{ij} \tag{4}$$

where Ω is the domain of the structure and

$$\delta_{ij} = \begin{cases} 1 & \text{if } i = j \\ 0 & \text{if } i \neq j \end{cases}.$$

Similarly, the eigenvalue problem of the post-damage system is written as

$$\bar{L}[\bar{W}(X)] - \bar{\lambda} M(X)\bar{W}(X) = 0 \tag{5}$$

and the corresponding eigensolutions are $\bar{\lambda}_i$ and $\bar{\phi}_i$, $i = 1,2,\ldots,$ which satisfy

$$\bar{L}[\bar{\phi}_i(X)] - \bar{\lambda}_i M[X]\bar{\phi}_i(X) = 0. \tag{6}$$

Equations (5) and (6) can be expanded based on the basis of assumptions listed in Section 4.1. Based on assumption (1), we have

$$\bar{L} = L + \Delta L. \tag{7}$$

The quantity ΔL represents the damage and is of interest to us. In a flaw detection problem, ΔL is unknown. From assumption (2), we can write

$$\begin{cases} \bar{\lambda}_i = \lambda_i + \Delta\lambda_i \\ \bar{\phi}_i = \phi_i + \Delta\phi_i \end{cases}. \tag{8}$$

Substituting (7) and (8) into (6), we get

$$(L + \Delta L)[\phi_i(X) + \Delta\phi_i] - (\lambda_i + \Delta\lambda_i)M[X](\phi_i(X) + \Delta\phi_i) = 0. \tag{9}$$

By subtracting eqn (2) from eqn (9), we obtain

$$L[\Delta\phi_i(X)] + \Delta L[\bar{\phi}_i(X)] - \lambda_i M(X)\Delta\phi_i(X) - \Delta\lambda_i M(X)\bar{\phi}_i(X) = 0. \tag{10}$$

On the basis of assumption (3), damage occurs within the domain of the system. The boundary conditions remain unchanged due to the damage, all the intact eigenfunctions, $\phi_i(X)$, $i = 1,2,\ldots,$ are comparison functions of the damaged structure. Thus, any eigenfunction of the damaged structure can be expressed as a linear combination of the intact eigenfunctions, i.e. the eigenfunction perturbation due to the damage can be expressed as

$$\Delta\phi_i(X) = \sum_{k=1}^{\infty} \beta_{ik}\phi_k(X), i = 1,2,\ldots, \tag{11}$$

where β_{ik}, $k = 1,2,\ldots,$ are constants.

Introducing (11) in (10), we get

$$L\left[\sum_{k=1}^{\infty} \beta_{ik}\phi_k(X)\right] + \Delta L[\bar{\phi}_i(X)] - \lambda_i M(X)\sum_{k=1}^{\infty} \beta_{ik}\phi_k(X) - \Delta\lambda_i M(X)\bar{\phi}_i(X) = 0 \tag{12}$$

Multiplying (12) by $\phi_i(X)$ and integrating over the structural domain Ω on both sides, we obtain

$$k_{ii}\beta_{ii} + \int_{\Omega} \phi_i(X)\Delta L[\bar{\phi}_i(X)]\,d\Omega - \lambda_i\beta_{ii}m_{ii} - \Delta\lambda_i\int_{\Omega} \phi_i(X)M(X)\bar{\phi}_i(X)\,d\Omega = 0 \tag{13}$$

where

$$k_{ii} = \int_\Omega \phi_i(X) L[\phi_i(X)]\, d\Omega = \lambda_i \tag{14}$$

$$m_{ii} = \int_\Omega \phi_i(X) M(X) \phi_i(X)\, d\Omega = 1 \tag{15}$$

are from the orthogonality conditions (3) and (4). Thus, eqn (13) can be simplified as

$$\int_\Omega \phi_i(X) \Delta L[\bar{\phi}_i(X)]\, d\Omega = \Delta\lambda_i \int_\Omega \phi_i(X) M(X) \bar{\phi}_i(X)\, d\Omega, \; i = 1,2,\ldots \tag{16}$$

Equations (16) relate the damage information "ΔL", eigenvalue changes $\Delta\lambda_i$, eigenfunction $\phi_i(X)$ of the undamaged structure, and the eigen function $\bar{\phi}_i(X)$ of the damaged structure in an integral equation form. If the damage is known, i.e. ΔL is known, the functions $\bar{\phi}_i(X)$ constitute the unknowns in equations in (16). In a flaw detection problem, which is an inverse problem, $\phi_i(X)$, $\bar{\phi}_i(X)$ and $\Delta\lambda_i$ are detected experimentally and ΔL is the unknown quantity that should be identified. The identification procedure and the use of curvature modes are discussed with a beam example in the next section.

4.3. *Beam example*

The experimental-data-based flaw detection is essentially an inverse structural dynamics problem, which estimates the flaw location and magnitude (or mechanical properties of the damaged structure) from the given structural dynamic response. In eqn (16), this inverse problem has been expressed in a form of an integral equation. Since the flaw information has been expressed implicitly in ΔL, which is actually a differential operator, it is difficult to seek a general solution directly from eqn (16). A more quantitative insight can be obtained by studying a specific case.

For beam cases, the operator L for an Euler–Benoulli beam can be written as

$$L = \frac{\partial^2}{\partial x^2}\left(EI\frac{\partial^2}{\partial x^2}\right). \tag{17}$$

For a single damage at $x = x_0$ case, the damage to the beam, ΔL, can be expressed in a perturbation of L as

$$\Delta L = \frac{\partial^2}{\partial x^2}\left(\alpha\delta(x-x_0)EI\frac{\partial^2}{\partial x^2}\right) \tag{18}$$

where α is stiffness loss factor; and δ is the Dirac's delta function.

Substituting (18) into (16) and integrating by parts, we get

$$\begin{aligned}
&\int_0^1 \phi_i(x)\frac{\partial^2}{\partial x^2}\left(\alpha\delta(x-x_0)EI\frac{\partial^2(\bar{\phi}_i(x))}{\partial x^2}\right)dx \\
&\quad = \phi_i(x)\frac{\partial}{\partial x}\left(\alpha\delta(x-x_0)EI\frac{\partial^2(\bar{\phi}_i(x))}{\partial x^2}\right)\Bigg|_0^1 \\
&\qquad - \frac{\partial(\phi_i(x))}{\partial x}\alpha\delta(x-x_0)EI\frac{\partial^2(\bar{\phi}_i(x))}{\partial x^2}\Bigg|_0^1 \\
&\qquad + \int_0^1 \alpha\delta(x-x_0)EI\frac{\partial^2(\phi_i(x))\partial^2(\bar{\phi}_i(x))}{\partial x^2 \quad \partial x^2}dx \\
&\quad = \Delta\lambda_i \int_\Omega \phi_i(X) M(X) \bar{\phi}_i(X)\, d\Omega, \quad i = 1,2,\ldots
\end{aligned} \tag{19}$$

Using the characteristics of the Dirac's delta function, one can easily simplify (19) as

$$\alpha EI\kappa_i(x_0)\bar{\kappa}_i(x_0) = \Delta\lambda_i \int_\Omega \phi_i(X)M(X)\bar{\phi}_i(X)\,d\Omega, i = 1,2,\ldots \tag{20}$$

where κ_i and $\bar{\kappa}_i$ are ith mode curvatures of pre- and post-damaged beams, respectively,

$$\kappa_i(x) = \frac{\partial^2\phi_i(x)}{\partial x^2}, \quad \bar{\kappa}_i(x) = \frac{\partial^2\bar{\phi}_i(x)}{\partial x^2}. \tag{21}$$

If there is a stiffness loss α at location x_0, the flaw information (the location x_0 and magnitude α) and the structural dynamic response (the curvature mode shapes κ_i and $\bar{\kappa}_i$, and frequencies $\Delta\lambda_i$) are related by (20). This relation can be easily expanded to a multi-site damage case. In a multi-site damage case, the ΔL can be expressed as

$$\Delta L = \sum_k \frac{\partial^2}{\partial x^2}\left(\alpha_k\delta(x-x_k)EI\frac{\partial^2}{\partial x^2}\right). \tag{22}$$

By substituting (22) into (16) and then integrating by parts, we can get

$$\sum_{k=1}^{n} \alpha_k EI\kappa_i(x_k)\bar{\kappa}_i(x_k) = \Delta\lambda_i \int_\Omega \phi_i(X)M(X)\bar{\phi}_i(X) \quad d\Omega, i = 1,2,\ldots \tag{23}$$

Equations (23) can be further simplified as

$$\sum_{k=1}^{n} \alpha_k EI\kappa_i(x_k)\bar{\kappa}(x_k) = \Delta\lambda_i\bar{m}_i, \quad i = 1,2,\ldots \tag{24}$$

where

$$\bar{m}_i = \int_\Omega \phi_i(X)M(X)\bar{\phi}_i(X)\,d\Omega, \quad i = 1,2,\ldots \tag{25}$$

As is shown in Section 6, the left-hand side of eqn (24) displays significant curvature change effect, whereas the value of $\bar{m}_i$, which depend on the displacement modes, is almost unity.

Based on eqn (24), a flaw detection scheme can be derived by using the combination of measured curvature mode shapes and frequencies. If there are n measuring stations, we can assign a stiffness loss factor, α_k, to each of the measuring location k. Here we assume that each measuring location is a damage location. If there is no damage at the measuring location, then the damage coefficient at this location is zero. From here on, the measuring location k and damage location k are used interchangeably.

If there are m modes of experimental data available for both intact and damaged structures, eqn (24) can be further expanded into a matrix form

$$[A]\{\alpha\} = [\bar{m}]\{\Delta\lambda\} \tag{26}$$

where

$[A]$ is an $m \times n$ matrix, and $A_{ij} = EI\kappa_i(x_j)\bar{\kappa}_i(x_j)$;

$\{\alpha\}$ is an $n \times 1$ vector, its elements stand for flaw magnitude at the measuring stations;

$\{\Delta\lambda\}$ is an $m \times 1$ vector, its elements are the eigenvalue differences between damaged and intact beams;

$[\bar{m}]$ is an $m \times m$ diagonal matrix, and $\bar{m}_{ii} = \bar{m}_i$.

If $m = n$, that is, the number of the measuring stations is equal to the number of the measured modes, then the $[A]$ matrix is square. Thus the solution $\{\alpha\}$ to eqn (26) is unique. In real problems, m is usually much larger than n. Numerical treatments are needed to obtain a reasonable solution for (26).

5. DETECTION PROCEDURES

In flaw detection procedure based on the proposed algorithm, if we can get a full rank square matrix **A** in eqn (26), we are able to detect the flaw location and magnitude easily by using conventional matrix inverse or many other standard numerical solution procedures. In practice, it is not realistic to get a full rank square matrix **A**. To get a full rank square matrix, we have to either reduce the measurement locations on the structure, which will reduce the measuring accuracy and detection credibility, or use high-order experimental modal analysis data, which are hard to obtain and low in accuracy. Usually, in a flaw detection setup, we have more measuring stations than the available experimental modal data, that is, we have an $m \times n$ rectangular matrix **A** in eqn (26). The number of the available experimental modes, m, is usually much smaller than the number of the measuring locations, n.

To seek a solution from eqn (26) with a rectangular maxtrix **A**, one can use mathematical manipulations like the pseudoinverse (or the Moore–Penrose inverse) (Pringle 1971). There are many numerical techniques available for effectively obtaining the pseudoinverse. One of the powerful methods is based on the "Singular Value Decomposition" technique (Klema and Laub 1980). The pseudoinverse techniques have been very useful in linear systems. These techniques are usually based on a minimization criterion. For example, the pseudoinverse based on the singular value decomposition technique simultaneously minimize the right hand side of eqn (26) and the solution norms (Biglieri and Yao, 1989). If we use a pseudoinverse technique directly in our flaw detection, the solution sought will tend to spread over the structural domain in order to satisfy the minimization criteria. Thus, a numerical treatment different from the conventional pseudoinverse techniques is required to increase the detection credibility.

Our numerical experiments, which will be discussed in the next section, have indicated that the curvature mode is much more damage sensitive than the regular displacement mode. Furthermore, the curvature mode change before and after the presence of the damage in the structure has a localized nature, that is, the curvature change is concentrated around the damage location. Based on these observations, an iterative solution procedure is constructed. In Fig. 1, we have shown the diagram of the solution procedure and the explanations for each step following.

The detection procedure includes the following main steps:

Step 1. *Initial guess.* In this step, the initial guess to the vector $\{\alpha\}$ in eqn (26), $\{\bar{\alpha}_0\}$, is taken as

$$\{\bar{\alpha}_0\} = \sum_{i=1}^{m} \{|\kappa_i - \bar{\kappa}_i|\} \tag{27}$$

which means the solution form takes the shape of the summation of the absolute value of the curvature difference before and after the damage. This is reasonable guess based on the observation that the curvature change has the damage localized nature.

Step 2. *DC elimination.* From Step 1, we can see that the initial guess is taken from the absolute value of the curvature change. Even though the curvature change correlated with the localized damage formation, the absolute value away from the damage location is small but not necessarily zero. Furthermore, the measurement noise may also be introduced into the curvature modal data. Thus, the initial guess based on equation (27) contains certain DC bias. Basically, this DC bias is unpredictable in a practical problem. To effectively eliminate the DC bias, we first define a noise level threshold: all the values in the initial guess less than fifteen percent of the maximum value are treated as noise. Then the DC bias, α_{av}, is taken as the average of the noise. A refined solution shape, $\{\hat{\alpha}\}$, is obtained by eliminating the DC bias, α_{av}, from the initial guess $\{\bar{\alpha}_0\}$:

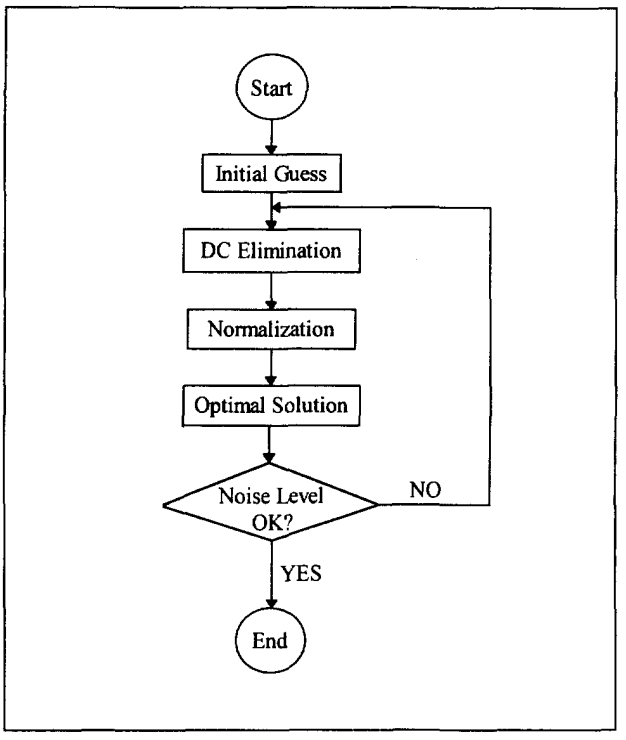

Fig. 1. Flaw detection diagram.

$$\{\hat{\alpha}\} = \{\bar{\alpha}\} - \alpha_{\text{av}} \tag{28}$$

Step 3. *Normalization.* This step is to select a scalar v such that

$$\min_{\forall v} \|[A]\{v\hat{\alpha}\} - [\bar{m}]\{\Delta\lambda\}\|$$

which yield

$$v = \frac{[A]\{\hat{\alpha}\} \cdot [\bar{m}]\{\Delta\lambda\}}{\|[A]\{\hat{\alpha}\}\|^2}$$

and the initial guess is scaled to

$$\{\alpha_0\} = v\{\hat{\alpha}\}. \tag{29}$$

Step 4. *Optimal solution.* The vector $\{\alpha_0\}$ from Step 3 is close to a solution under a minimum norm sense, but $\{\alpha_0\}$ does not necessarily satisfy eqn (26) exactly due to the noise. The purpose of this step is to find a solution $\{\alpha\}$ for eqn (26) in the neighborhood of $\{\alpha_0\}$, i.e.

$$\min_{\forall([A]\{\alpha\} = \{\Delta\lambda\})} \|\{\alpha\} - \{\alpha_0\}\|.$$

Using Lagrangian multiplier Λ, we construct a cost function J as

$$J = \{\alpha-\alpha_0\}^T\{\alpha-\alpha_0\} + \{\Lambda\}^T([A]\{\alpha\} - [\bar{m}]\{\Delta\lambda\}). \tag{30}$$

By minimizing J with respect to $\{\alpha\}$, we get

$$\begin{bmatrix} I_{n\times n} & A^T_{n\times m} \\ A_{m\times n} & O_{m\times m} \end{bmatrix} \begin{Bmatrix} \alpha_{n\times 1} \\ \Lambda_{m\times 1} \end{Bmatrix} = \begin{Bmatrix} \alpha_{0_{n\times 1}} \\ ([\bar{m}]\{\Delta\lambda\})_{m\times 1} \end{Bmatrix} \tag{31}$$

where $I_{n\times n}$ stands for the identity matrix. Equation (31) can be solved easily by standard methods.

Step 5. *Noise level OK?* Generally, we are able to get a satisfactory solution from eqn (26). For high noise level cases, the solution can be improved by going back to Step 2.

6. EXAMPLES

6.1. *Numerical simulations*

To verify the flaw detection algorithm derived above, a simply-supported beam with uniform bending stiffness EI_0 and length L is numerically simulated. Two damage cases were tested. The stiffness losses of the single damaged and double damaged cases are shown in Fig. 2(a), (b). The boundary value problem is solved for the intact beam first. Then the damaged beam eigenvalue problem is solved by using the Rayleigh–Ritz method with the intact beam eigenfunctions as a trial family. In Fig. 3, the first three displacement modes, curvature modes and the shape differences due to a single damage are shown. Similarly, in Fig. 4, we have shown the first three modes of the double damage case. From Figs 3 and 4, two points are clearly seen:

(1) curvature modes are more sensitive to the presence of damage in the beam;

(2) curvature modes give out more localized information. The influence of the damage to the displacement mode shapes tends to spread all over the structure, while the influence on the curvature modes is concentrated near the damage locations.

6.1.1. *Comparison of the effect of damage on curvature and displacement modes.* Before we verify the detection algorithm, it is worthy numerically to check the effects of damages on the displacement mode shapes and curvature mode shapes. Using the generated data for intact and damaged beams, we examined quantities of

$$\bar{m} = \int_\Omega \phi_i(X)M(X)\bar{\phi}_i(X)\,d\Omega, \quad \Delta\bar{k} = \int_\Omega \phi_i(X)\Delta L[[\phi_i(X)]\,d\Omega,$$

and

$$\Delta k = \int_\Omega \phi_i(X)\Delta L[\phi_i(X)]\,d\Omega$$

for single and double stiffness loss cases and listed in Tables 1 and 2, where error is defined as $(\Delta\bar{k}-\Delta k)/\Delta k \times 100\%$.

From Tables 1 and 2, it is clearly seen that effects of the damage on the displacement mode shapes are very small. In practical damage detection application, assuming $\bar{m}_i = 1$ in eqn (24) should not induce any significant error. Whereas, the effect of the damage on curvature modes may be significant, for example, interchanging the intact and damaged curvature mode shapes in the left-hand side of (16) (or in (24)) in the two cases can cause up to 25% error.

6.1.2. *Validation of detection algorithm.* To verify the detection algorithm (26), two measuring configurations are simulated. In the first configuration, we assume that there are 10 sensors on the beam and measuring data of the first 10 modes are available. In this case,

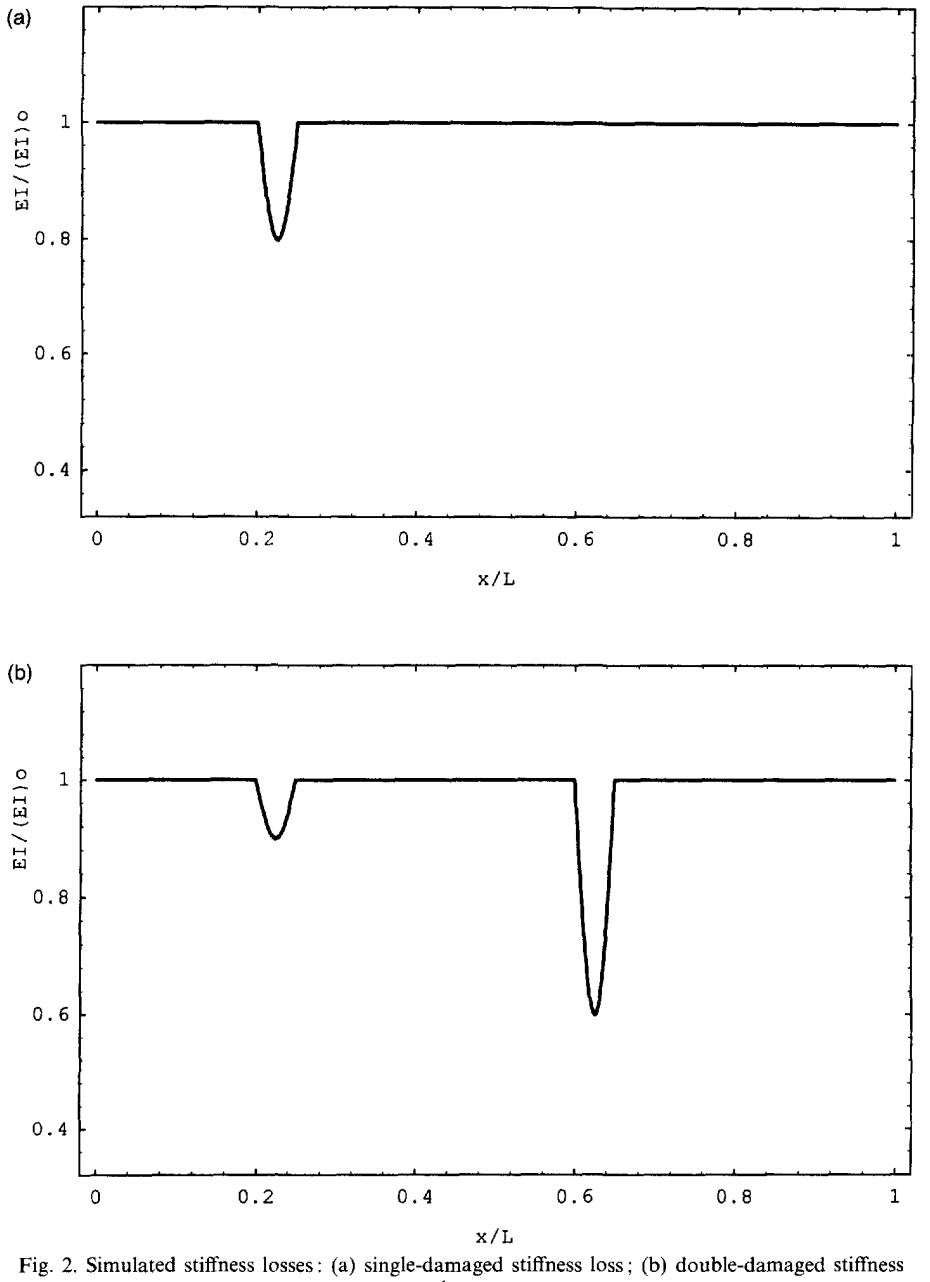

Fig. 2. Simulated stiffness losses: (a) single-damaged stiffness loss; (b) double-damaged stiffness loss.

Table 1. Effects of damages on mode shapes, single-damage case

Mode no.	$\bar{m}$	$\Delta\bar{k}$	Δk	Error (%)
1	0.999996	0.619167	0.523343	15.48
2	0.999970	22.5090	19.2705	14.39
3	0.999961	83.5577	72.5582	13.16
4	0.999989	40.2181	35.0562	12.83
5	0.999964	150.110	129.193	13.93

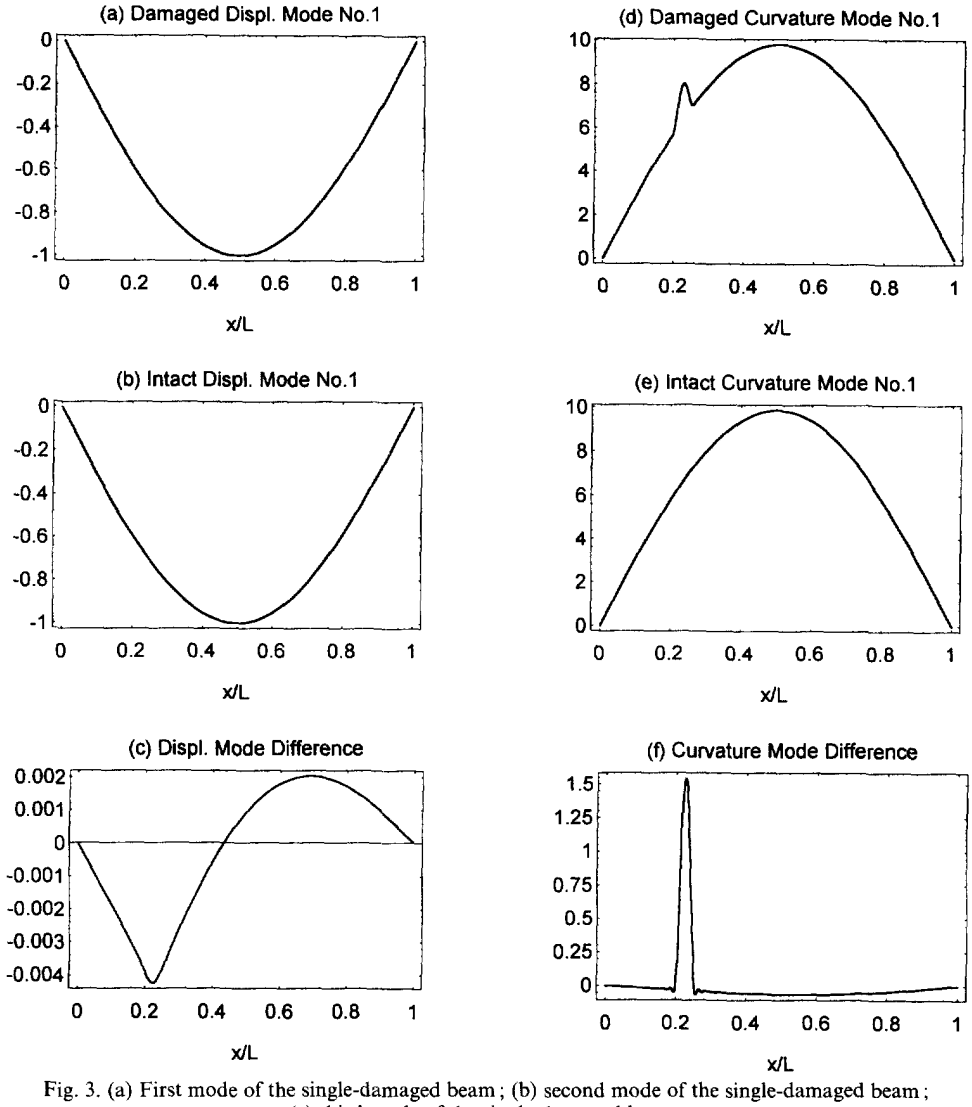

Fig. 3. (a) First mode of the single-damaged beam; (b) second mode of the single-damaged beam; (c) third mode of the single-damaged beam.

Table 2. Effects of damages on mode shapes, double-damage case

Mode no.	$\bar{m}$	$\Delta\bar{k}$	Δk	Error (%)
1	0.999983	1.03098	0.79047	22.36
2	0.999927	17.3730	14.5962	15.98
3	0.999908	49.1550	44.0058	10.48
4	0.999626	232.851	173.353	25.55
5	0.999964	156.609	129.193	17.51

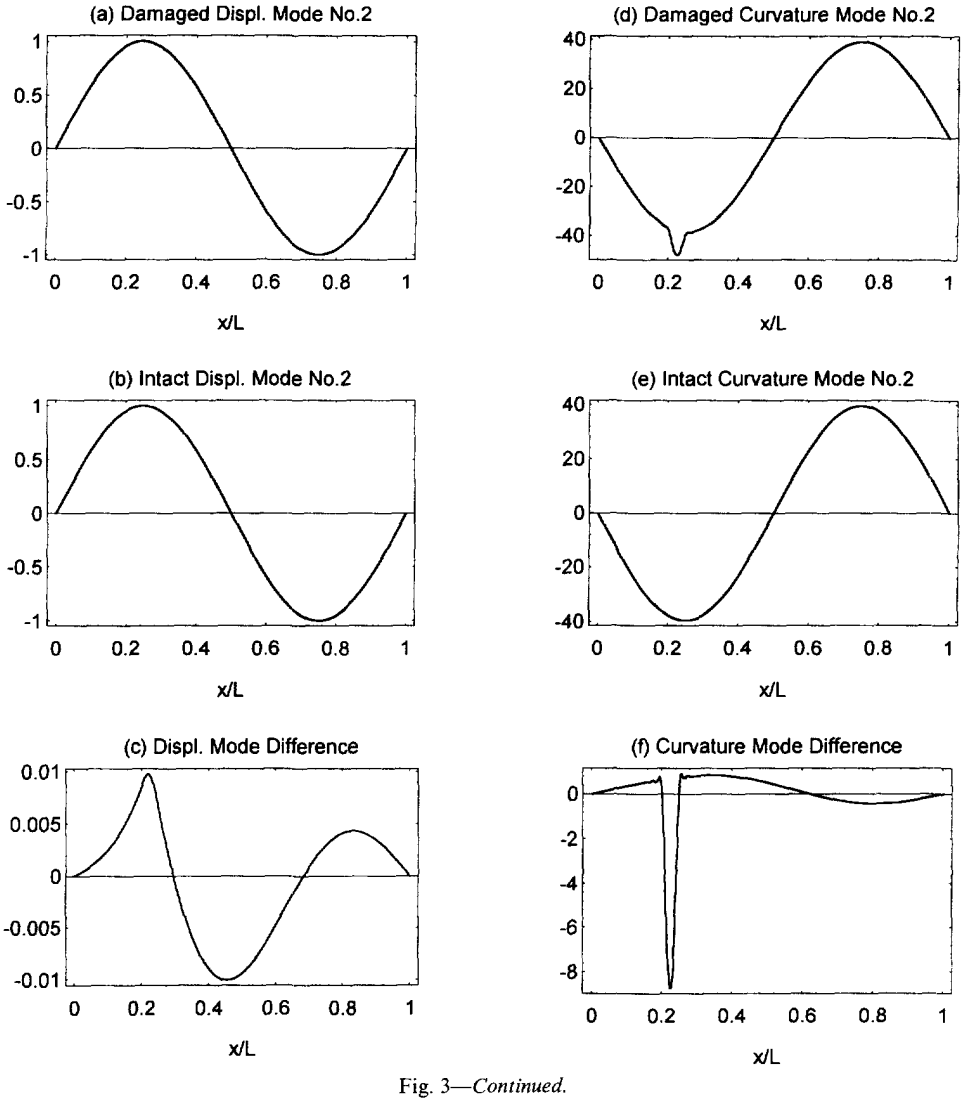

Fig. 3—*Continued.*

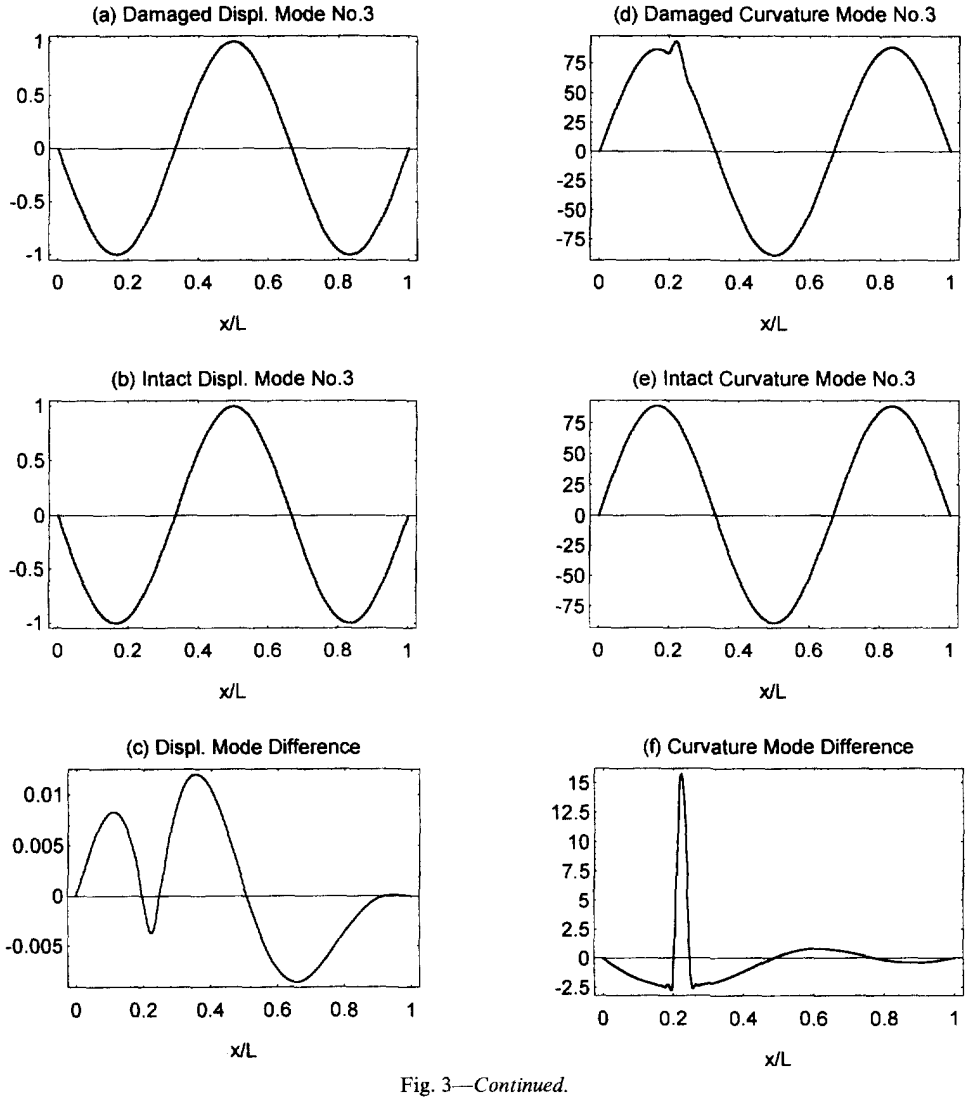

Fig. 3—*Continued.*

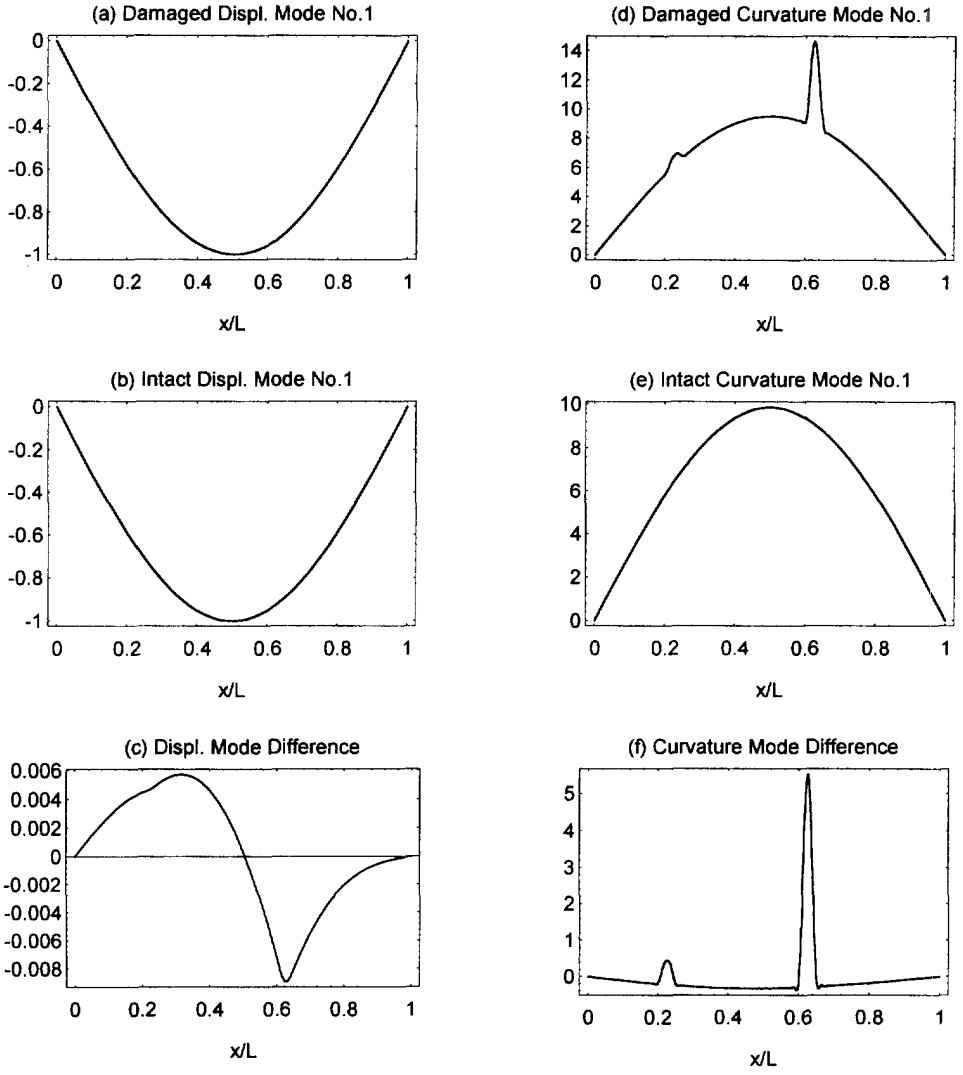

Fig. 4. (a) First mode of the double-damaged beam; (b) second mode of the double-damaged beam; (c) third mode of the double-damaged beam.

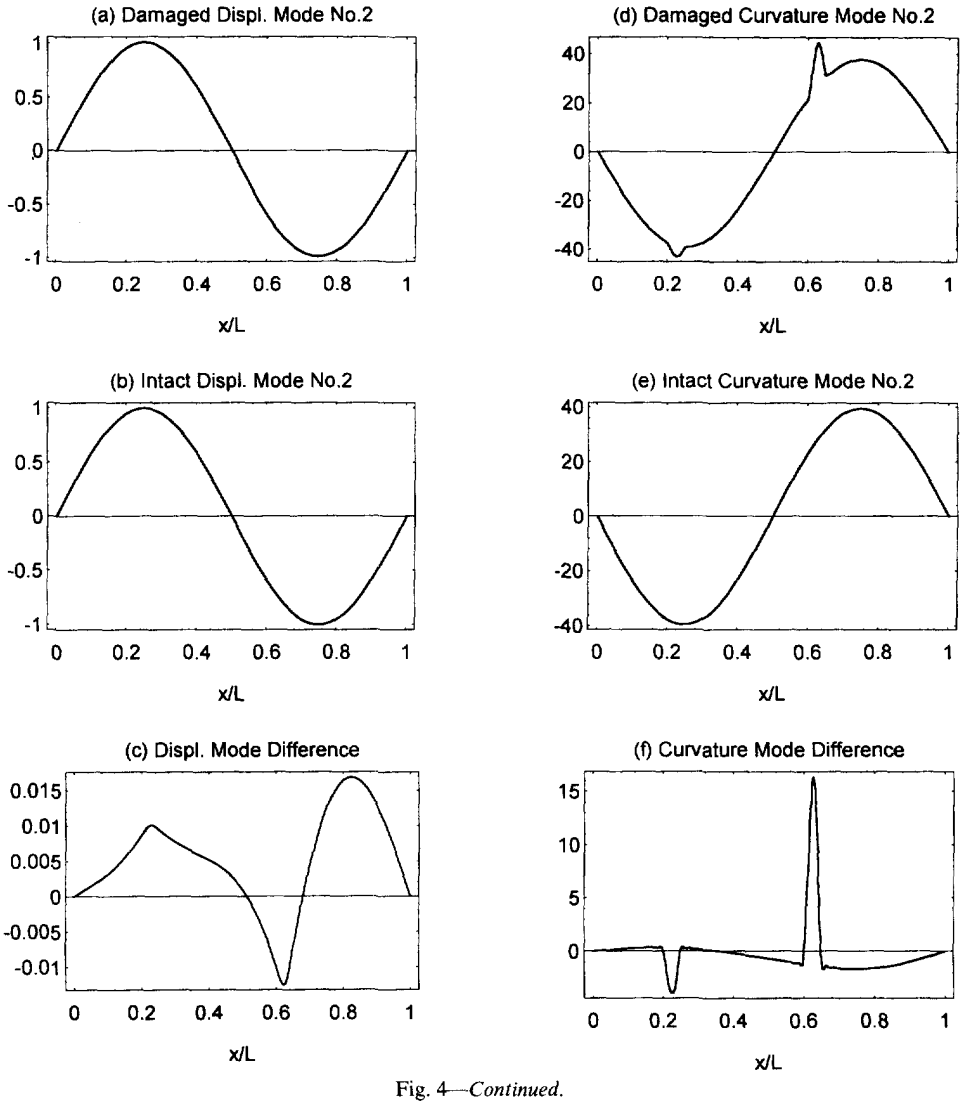

Fig. 4—*Continued.*

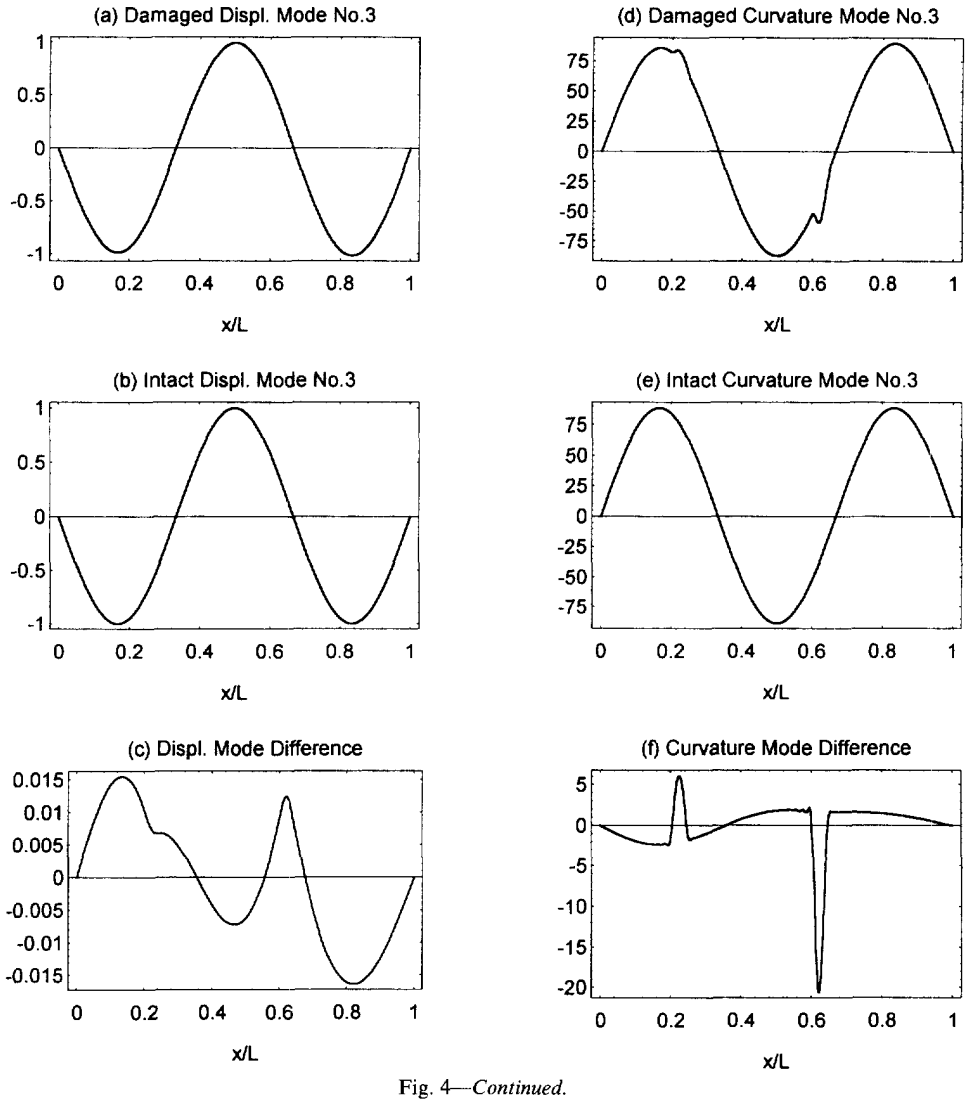

Fig. 4—*Continued.*

matrix **A** in the detection eqn (26) is a square matrix with full rank, thus the detection solution is unique. In Figs 5 and 6, we have shown the full rank solutions for the single-damaged beam and double-damaged beam, respectively. In Figs 5 and 6, the solid lines indicate the simulated stiffness distribution of the damaged beams, while the dashed lines represent the detection results. It is seen from these figures that the damage locations are identified precisely. The detected damage magnitudes are accurate in the integration sense.

In practice, the number of experimentally obtained modes is usually smaller than the number of measuring stations on the structure, thus matrix **A** in eqn (26) is rectangular. There are more unknowns than equations in (26). In this case, the solution is not unique. We have to use numerical procedures to solve the detection solutions. In Figs 7 and 8, we have shown the solutions following the solution steps described in Section 5. In this configuration, we assumed there were 20 measuring locations on the beam. Only the first five modes were used in detection.

6.2. *Experimental examples*

A brief summary of the validation of the theory by conducting experiments is discussed in this section. Twelve-ply woven glass cloth and epoxy matrix composite beam specimens were manufactured and tested. Damages were introduced by saw-cut and hammer impact (see Fig. 9). Experimental modal analyses were first conducted on intact beam specimens.

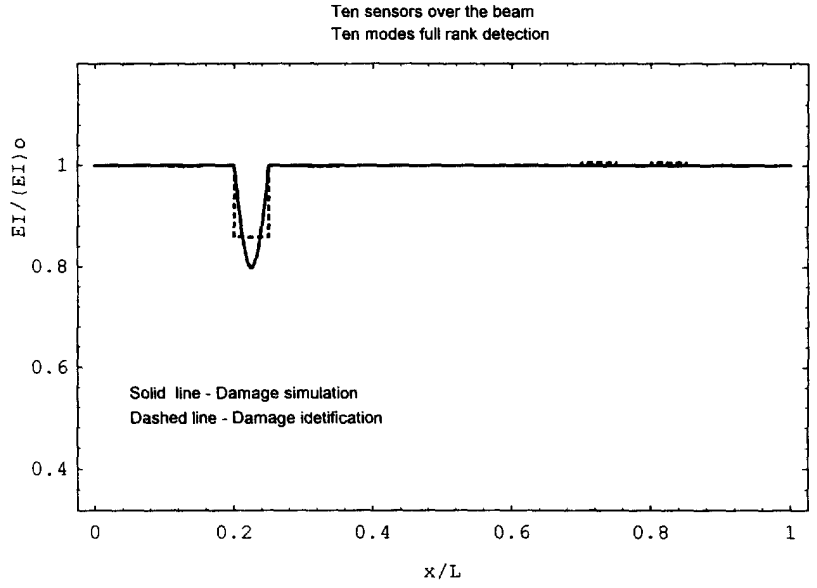

Fig. 5. Single-damaged beam full rank detection.

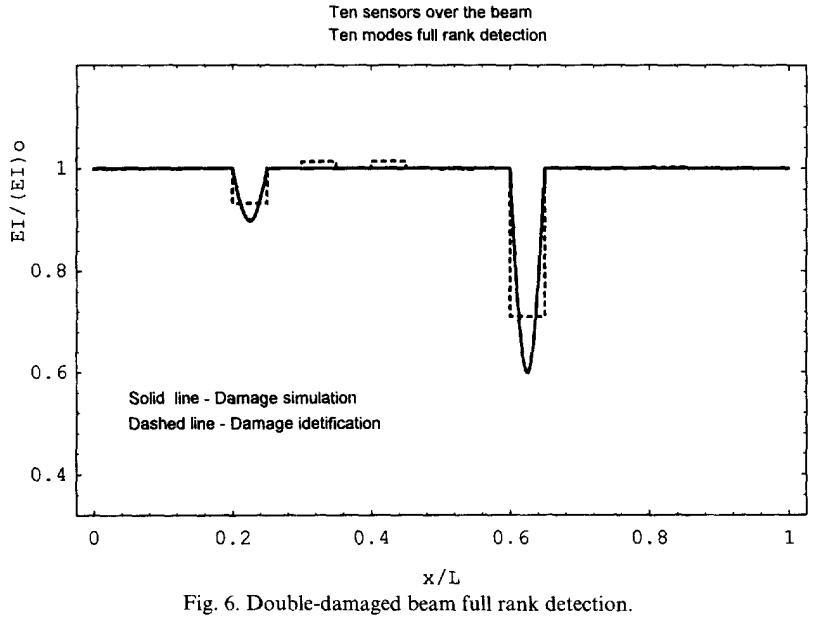

Fig. 6. Double-damaged beam full rank detection.

The intact curvature modes were recorded for reference. To introduce the saw-cut damage, the intact beam was cut at 8.75 cm from the cantilever end. The depth of the through width saw-cut is about half of the specimen thickness. Experimental modal analysis was then conducted on the saw-cut damaged specimen to obtain the curvature modal shape. For impact damage case modal analysis was carried out for the intact beam first. The damage was introduced by hammer impacts in the region of 10–12.5 cm from the fixed end. The impact damaged specimen was then used in modal analysis experiment to obtain the curvature mode shapes.

In the modal analyses, a PVDF (Polyvinylidenefluoride) sensor was used to detect the response, and a PCB hammer input was used to excite the specimens. A GENRAD modal analysis system was used for data acquisition and modal analysis. Typical PVDF film thickness ranges from 20 to 100 μm, thus, in practice, we can neglect the sensor thickness without introducing significant amount of error. With the assumptions that all in-plane strains are negligible, we have a general charge-deformation relation for a plate as

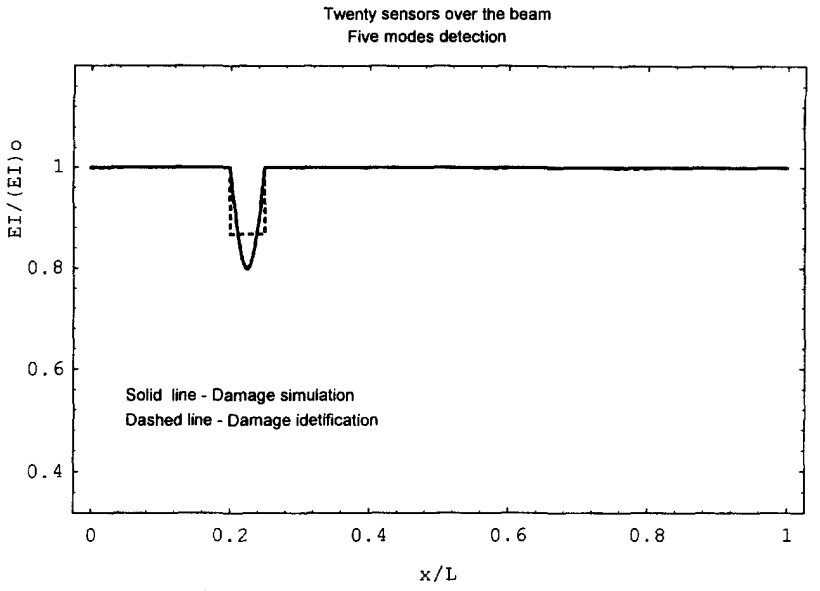

Fig. 7. Single-damaged beam iterative detection.

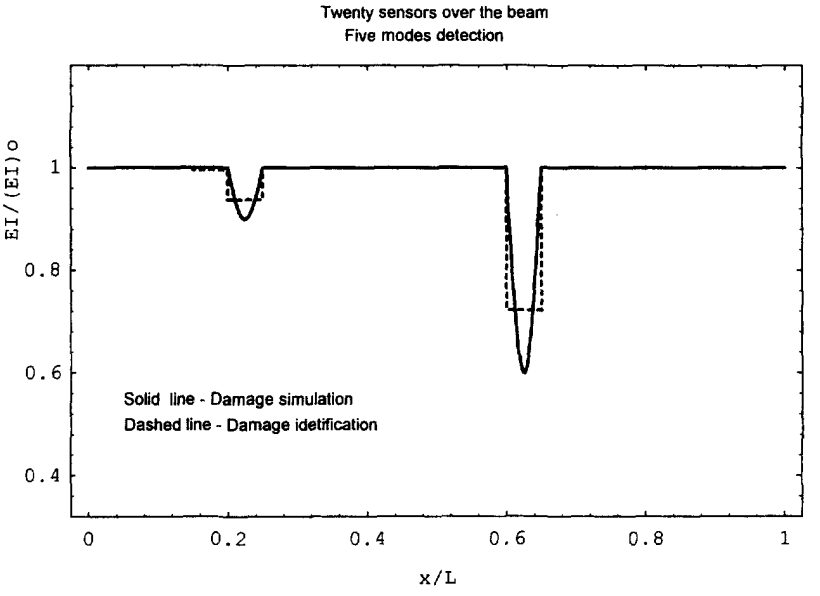

Fig. 8. Double-damaged beam iterative detection.

$$q(t) = -Gh\int_S \left(e_{31}\frac{\partial^2 w}{\partial x^2} + e_{32}\frac{\partial^2 w}{\partial y^2} + 2e_{36}\frac{\partial^2 w}{\partial x \partial y}\right)\mathrm{d}x\,\mathrm{d}y \tag{32}$$

where q is the signal received by the A/D converter; G is the total electronic circuit gain; h is the distance from the sensor surface to the structure local neutral plane; S is the sensor area; w is the flexural displacement of the plate; e_{ij}s are the piezo constants of the PVDF film. Usually, in PVDF the e_{36} is negligibly small and e_{31} and e_{32} can be made to equal, thus eqn (32) is reduced to

$$q(t) = -Ghe_{31}(\kappa_{xx} + \kappa_{yy})S \tag{33}$$

where κ_{xx} and κ_{yy} are the averaged local curvatures in x and y directions. In beam cases, equation (33) can be further simplified as

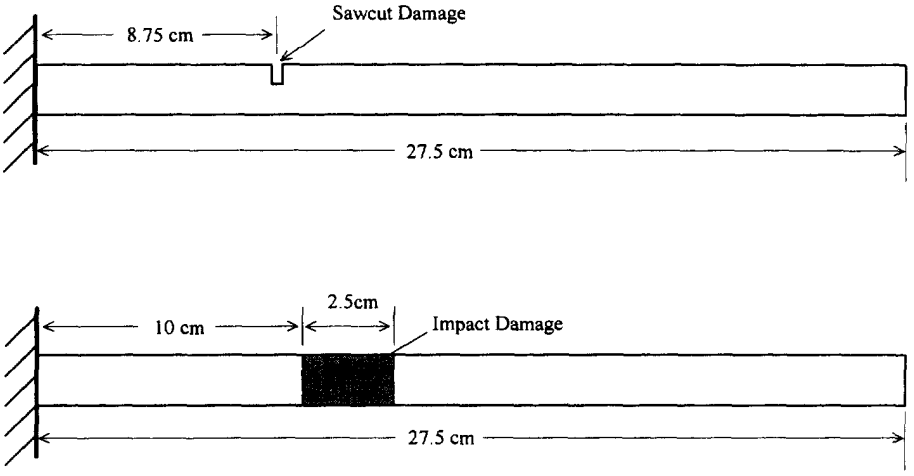

Fig. 9. Saw-cut damage and hammer impact damage.

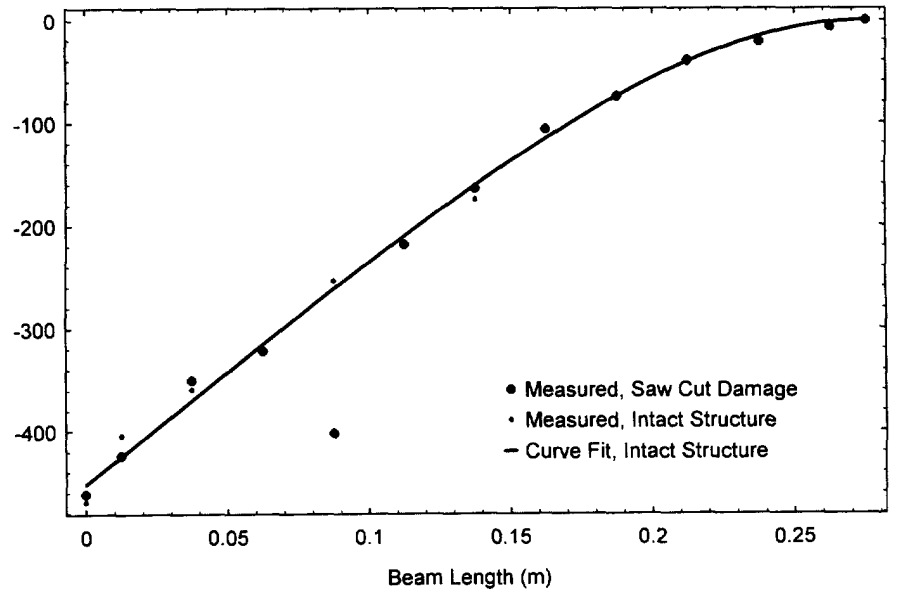

Fig. 10. Measured first curvature mode (mass normalized) of the beam with saw-cut damage, intact and the corresponding curve-fit.

$$q(t) = -Ghe_{31}\kappa_{xx}S. \tag{34}$$

Equations (33) and (34) indicate that the PVDF sensor output is proportional to the local curvatures.

From the numerical simulation analysis, it is indicated that the sensitivity of the curvature mode shapes to the stiffness loss damage is higher than that of the displacement mode shapes. Furthermore, the stiffness loss damage reflected in the curvature modes is local in nature. The results obtained from experiments support the numerical conclusions. In Figs 10 and 11, the measured first two curvature modes of the saw-cut damaged beam and its corresponding intact beam, together with the curve-fit result, are shown. It is clearly seen that the curvature modes of the damaged beam have an abrupt change at the damage location (8.75 cm from the left end).

Using the curvature mode shapes of the intact and the saw-cut damaged specimens, we construct the matrix $[A]$, where $A_{ij} = EI\kappa_i(x_j)\bar{\kappa}_i(x_j)$, in eqn (26). From Table 3 we can construct the vector $\{\Delta\lambda\}$ in eqn (26), where $\Delta\lambda_i$ is the eigenvalue difference between the saw-cut damaged beam and the intact beam. Following the detection procedures proposed in Section 4, we conduct the flaw detection and the detection result is shown in Fig. 12.

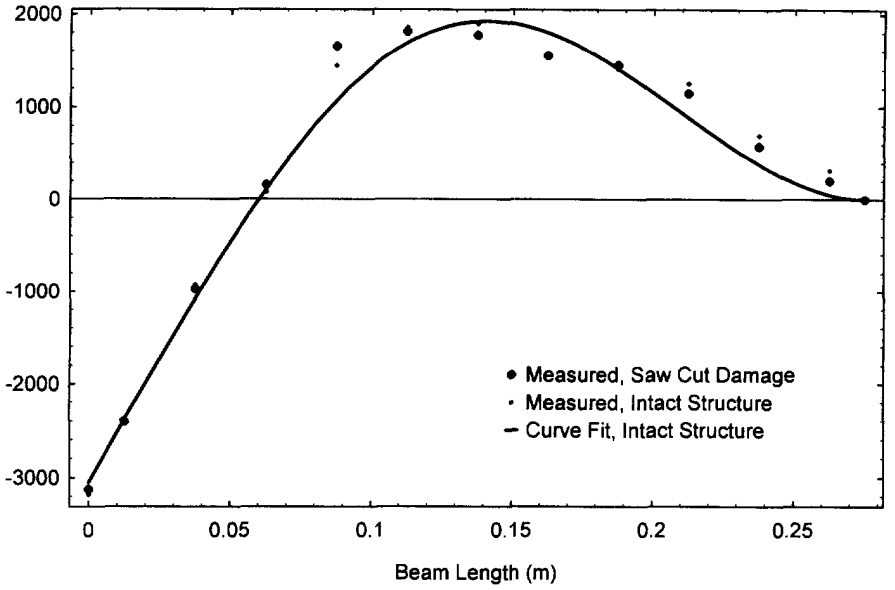

Fig. 11. Measured second curvature mode (mass normalized) of the beam with saw-cut damage, intact and the corresponding curve-fit.

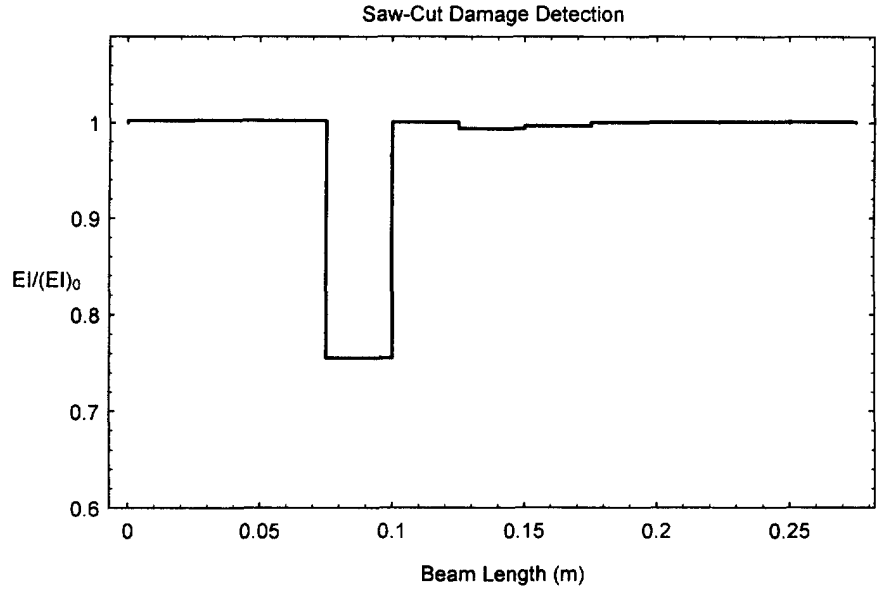

Fig. 12. Detection results of the saw-cut damaged beam.

Similarly, we conducted the flaw detection for the impact damaged case. The curvature and frequency information of the hammer impact damaged beam and the corresponding intact beam are shown in Figs 13–14 and Table 4. The sensitivity and the locality of curvature modes to the impact damage are also revealed in this case. The detection results are displayed in Fig. 15.

7. CONCLUSIONS

In this paper, a flaw detection algorithm is derived that use only experimental data. The basic assumptions used in the derivations are: the damage can be described as a stiffness loss in the structure; the damage occurs in the structure and the boundary conditions remain unchanged after the damage; the structure was stable before the damage occurred; the presence of the damage in the structure does not alter the stability of the structure. Based

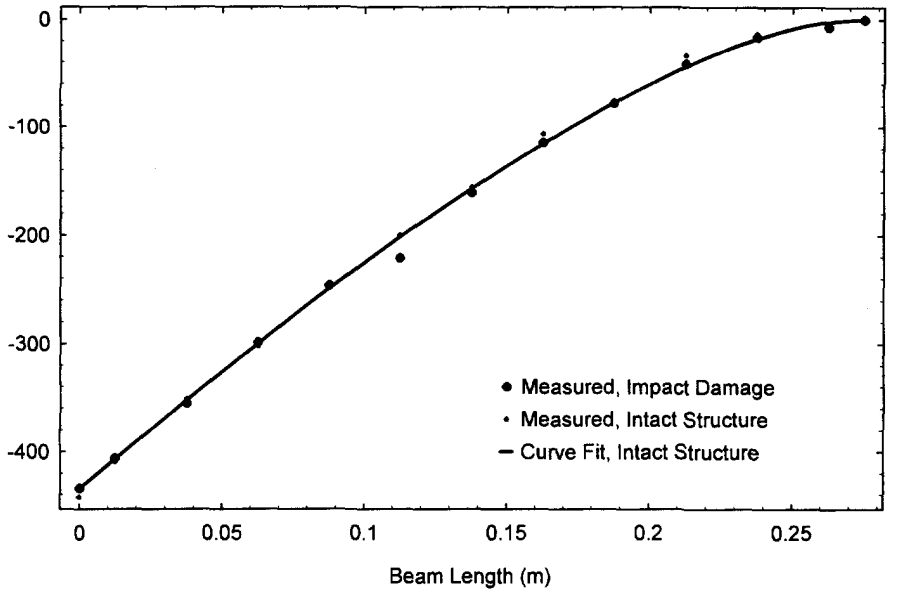

Fig. 13. Measured first curvature mode (mass normalized) of the beam with impact damage, intact and the corresponding curve-fit.

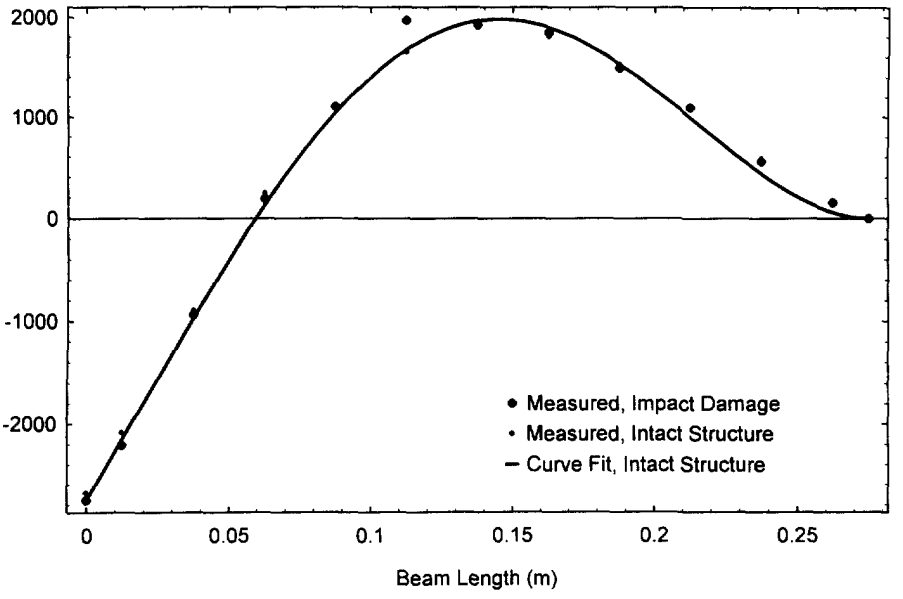

Fig. 14. Measured second curvature mode (mass normalized) of the beam with impact damage, intact and the corresponding curve-fit.

on these assumptions, we derived an integral equation that relates the damage parameters, modes of the undamaged structure, modes of the damaged structure, and natural frequency changes. The integral equation was then used to derive a flaw detection algorithm. The following are the conclusions drawn from this research:

(1) A flaw detection algorithm has been derived which has a systematic mathematical background in a form of integral equation based on fundamentals of mechanics without using empirical judgment during the flaw detection.
(2) The curvature changes induced due to damages cannot be neglected.
(3) The detection algorithm uses the eigenvalue as well as eigenfunction information of the system, which is expected to have better detection performance in comparison with those detection methods use only partial system information such as eigenvalue information or eigenfunction information alone.

Table 3. Frequency information of the saw-cut damaged and intact beams (Hz)

Mode no.	1	2	3	4
Saw-cut damaged	23.443	150.729	414.189	829.636
Intact	23.966	152.258	425.879	830.007

Table 4. Frequency information of the impact damaged and intact beams (Hz)

Mode no.	1	2	3	4
Impact damaged	25.996	162.400	462.642	904.907
Intact	27.313	169.443	477.673	935.420

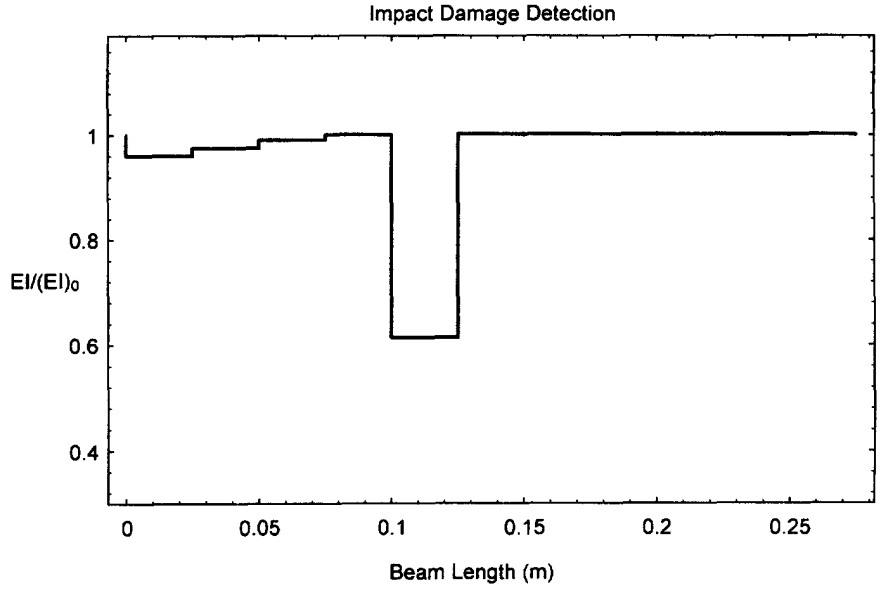

Fig. 15. Detection results of the impact damaged beam.

(4) The input to the flaw detection uses only experimental data. System modeling is not required in flaw detection.
(5) Damage locations and the corresponding damage severities can be identified simultaneously.

REFERENCES

Adams, R. D., Walton, D., Flitcroft, J. E. and Short, D. (1975). Vibration testing as a non-destructive test tool for composite materials. *Composite Reliability, ASTM, STP*, **580,** 159–175.

Adams, R. D., Cawley, P., Pye, C. J. and Stone, B. J. (1978). A vibration technique for non-destructively assessing the integrity of structures. *Journal of Mechanical Engineering Science*, **20**(2), 93–100.

Armon, D., Ben-Haim, Y. and Braun, S. (1991). Crack detection in beams by rank-ordering of eigen-frequency shifts. *IFAC Symposia Series No. 6, IFAC/IMACS Symposium on Fault Detection, Supervision and Safety for Technical Processes—SAFEPROCESS'91*, pp. 153–158. Pergamon, Tarrytown, NY.

Biglieri, E. and Yao, K. (1989). Some properties of singular value decomposition and their applications to digital signal processing. *Signal Processing*, **18,** 277–289.

Cawley, P. and Adams, R. D. (1979a). The localization of defects in structure from measurements of natural frequencies. *Journal of Strain Analysis*, **2,** 49–57.

Cawley, P. and Adams, R. D. (1979b). A vibration technique for non-destructive testing of fiber composite structures. *Journal of Composite Materials*, **13**(3), 161–175.

Cempel, C., Natke, H. G. and Ziolkowski, A. (1992). Application of transformed normal modes for damage location in structures. *Structural Integrity Assessment*, ed. P. Stanley, pp. 246–255. Elsevier, Oxford.

Collins, J. D., Hart, G. C., Hasselman, T. K. and Kennedy, B. (1974). Statistical identification of structures. *AIAA Journal*, **12**(2), 185–190.

Frankle, R. S. (1993). Practical applications of multimodal NDT data. *Proceedings of SPIE—The International Society for Optical Engineering*, Vol. 1785, pp. 184–195.

Griffin, S. F. and Sun, C. T. (1991). Health monitoring of dumb and smart structures. *28th Annual Technical Meeting of SES.*

Kabe, A. M. (1985). Stiffness matrix adjustment using mode data. *AIAA Journal*, **28**(9), 1431–1436.

Klema, V. C. and Laub, A. J. (1980). The singular value decomposition : its computation and some applications. *IEEE Transactions on Automatic Control*, **AC-25**(2), 164–176.

Kreier, P., Gribi, M., Durocher, J. M., Hay, D. R., Pellrtier, A. and Edelmann, X. (1993). Computer integrated testing. *European Journal of Non-Destructive Testing*, **2**(3), 96–99.

Lee, B. T., Sun, T. C. and Liu, D. (1987). An assessment of damping measurements in the evaluation of integrity of composite beams. *Journal of Reinforced Plastics and Composites*, **6**, 114–125.

Lim, T. W. (1995). Structural damage detection using constrained eigenstructure assignment. *Journal of Guidance, Control and Dynamics*, **18**(3), 411–418.

Lin, R. M. (1993). Analytical model improvement using modified IEM. *Proceedings of the International Conference on Structural Dynamics Modeling*, pp. 181–194. National Agency for Finite Element Methods and Standards, Glasgow, Scotland.

Luo, H. (1996). Damage detection and health monitoring of structures using dynamic response and neural network techniques. Ph.D. dissertation, Georgia Institute of Technology.

Manning, R. A. (1994). Structural damage detection using active members and neural networks. *AIAA Journal*, **32**(6), 1331–1333.

Mantena, R., Gibson, R. F., and Place, T. A. (1986). Damping capacity measurements of degradation in advanced materials. *SAME Quarterly*, **17**(3), 20–31.

Minas, C. and Inman, D. J. (1990). Matching finite element models to modal data. *Journal of Vibration and Acoustics*, **112**, 84–88.

Pabst, U. and Hagedorn, P. (1993). On the identification of localized losses of stiffness in structures. *American Society of Mechanical Engineers*, **DE 59**, 99–104.

Pandey, A. K., Biswas, M. and Samman, M. M. (1991). Damage detection from changes in curvature mode shapes. *Journal of Sound and Vibration*, **145**(2), 321–332.

Pringle, R. M. (1971). *Generalized Inverse Matrices with Applications to Statistics.* Griffin's statistical monographs and courses, no. 28, Griffin, London.

Rhim, J. and Lee, S. W. (1995). A neural network approach for damage detection and identification of structures. *Computational Mechanics*, **16**, 437–443.

Rodden, W. P. (1967). A method for deriving structural influence coefficients from ground vibration test. *AIAA Journal*, **5**(5), 991–1000.

Worden, K., Ball, A. D. and Tomlinson, G. R. (1993). Fault location in a framework structure using neural networks. *Smart Materials and Structures*, **2**, 189–200.

Wu, X., Ghaboussi, J. and Garrett, J. H. Jr (1992). Use of neural networks in detection of structural damage. *Computers and Structures*, **42**(4), 649–659.

Zimmerman, D. C. and Kaouk, M. (1992). Eigenstructure assignment approach for structural damage detection. *AIAA Journal*, **30**(7), 1848–1855.

Ziolkowski, A. (1992). Application of transformed normal modes for damage location in structures. *Structural Integrity Assessment*, P. Stanley. Elsevier, Oxford.